

## Aerodynamic performances improvement of NACA 4415 profile by passive flow control using vortex generators

H. Hares<sup>1</sup>, G. Mebarki<sup>2\*</sup>, M. Brioua<sup>3</sup> and M. Naoun<sup>4</sup>

<sup>1</sup> LICEGS Laboratory, Mechanical Engineering Department, Faculty of Technology, Batna 2 University, Algeria

E-mail: hocinehares91@gmail.com

<sup>2</sup> LESEI Laboratory, Mechanical Engineering Department, Faculty of Technology, Batna 2 University, Algeria

E-mail: g.mebarki@univ-batna2.dz

<sup>3</sup> LICEGS Laboratory, Mechanical Engineering Department, Faculty of Technology, Batna 2 University, Algeria

E-mail: m.brioua@univ-batna2.dz

<sup>4</sup> Mechanical Engineering Department, Faculty of Technology, Batna 2 University, Algeria

E-mail: mnaoun@yahoo.fr

*\*corresponding author*

### Abstract

Improvement of the airfoil NACA 4415 aerodynamic performances by flow control using a passive technique was achieved in this study. Gothic-shaped vortex generators were added at the profile upper surface. Vortex Generators (VG) were used to avoid boundary layer separation at the profile trailing edge, thus reducing the drag force and improving aerodynamic performances. A numerical simulation with fluent code was performed. A parametric study was carried out to determine optimal disposition and dimensions of the VG. Six VG parameters were tested; thickness (E), height (H), length (L), aspect ratio (r), incidence angle ( $\alpha$ ) and the VG position relative to the chord of the profile (XVG). The results show an increase in the lift coefficient for the profile with vortex generators in the range of high attack angles. Optimal dimensions and positions of the VG were obtained.

**Keywords:** Aerodynamic performances, Lift coefficient, Drag coefficient, Vortex generators, Numerical simulation

### 1. Introduction

Flow control is important in aerodynamics. It is used to manipulate flows by passive or active techniques to improve the aerodynamic airfoils performances (lift augmentation, drag reduction, noise minimization and avoiding or postponing boundary layer separation). The active methods involve external power, whereas the passive methods use surface or geometrical modifications of the flow by incorporating inserts or additional devices (Mebarki & al 2016). Avoiding boundary layer separation leads to preventing pressure losses in the trailing edge of airfoils reducing the

drag force (Tebbiche 2016). The improvement of the lift force for high incidence angle and low velocity lead to the reduction of the runway length. This is particularly interesting for aircraft in areas with low aeronautical infrastructure potential (Lu et al. 2011). Vortex generators (VG) are widely used in passive control method to prevent flow separation on airfoils. These devices are small plates with different shapes and sizes at an angle to the incoming flow. The VG are oriented so they create longitudinal vortices, which enhance mixing high-momentum fluid from the outer flow down into the boundary layer near the surface (Wang et al. 2017). Since the final configuration cannot be changed during their application, they have to be implemented in an optimum position. Finding an optimum position is an important point for the aerodynamic performances of passive flow control system (Moshfeghi et al 2017). In the last decade, several researches have been devoted to passive flow control methods using vortex generators to improve the aerodynamic performances of airfoils (Lu et al. 2011, Cai et al. 2017, Mdouki 2017, Moghaddam1 et al. 2017 and Ahmed et al. 2017). Zhen et al. (2011) investigated experimentally and numerically the effects of passive vortex generators on Aludra unmanned aerial vehicle (UAV). An array of VG has been attached on Aludra UAV's wing and good agreement was obtained between experimental and numerical results. Their parametric study shows that higher maximum lift coefficient is achieved when the VG are placed near the separation point. Fouatih et al. (2016) provides an experimental optimization of a NACA 4415 airfoil equipped with vortex generators to control the flow separation. A new configuration including micro generators behind the conventional VG was also investigated as a potentially interesting solution. The results show that triangular shape vortex generators are best suited to control boundary layer separation. It was found that micro vortex generators are very effective to control the flow. Tebbiche et al. (2015) studied the effect of a new VG configuration, delta wing shape, placed on line on the suction surface of a curved profile (NACA 4412). The experimental study conducted in a wind tunnel shows an improved lift coefficient with an increase of 20% and one degree delay of the stall incidence. The prediction of the flow patterns around the vortex generators and the effects of changing their position and the incidence angle of the wind relative to the profile have been studied by several researchers (Forster et al. 2014 and Benazieb et al. 2015). The results indicate that the knowledge of these effects could be successfully applied to other wing profiles and designs. Vidhyasri et al. (2017) used vortex generators to reduce the fuel consumption and improve the vehicles driving performances by reducing the drag force. Various shapes of vortex generators (gothic, parabolic, ogive, rectangular and triangular) were designed and analyzed using CFD solver. Optimal results were obtained. Flow control using "V" shape vortex generators was investigated experimentally by Tebbiche et al. (2014). The VG were placed at the suction side of Naca 0015 profile in order to minimize the induced drag. Optimal drag coefficient was obtained taking into account several parameters such as the VG height, the position from the leading edge and the aperture. The effects of VG attached at different locations and at various attack angles have been studied by Gopinathan et al. (2015), Kumar et al. (2016) and Agarwal et al. (2016). They found that at small attack angles, the VG have insignificant effects with a small decrease in the lift force and a small increase in the drag force. However, at larger attack angles the lift force increases and the drag force decreases significantly. Belamadi et al. (2016) have also found that, the passive control system using VG improves aerodynamic performance only over a specific range of attack angles. Tebbiche et al. (2014) studied the flow control using a new vortex generators shape with counter-rotating vortices, obtained by modifying a configuration already investigated. An optimized geometry form in this paper was found by experimental design method. The results show an increase in the relative lift force estimated at about 14% and a decrease in the drag force about 16%.

In this study, a passive technique was used to control the separation of the boundary layer using vortex generators. Gothic-shaped vortex generators were attached at the upper surface (extrados) of NACA 4415 profile to improve its aerodynamic performances (lift augmentation and drag reduction). The Newtonian, incompressible and three dimensional Reynolds-averaged Navier-

Stokes equations were adopted in this study. The Realizable k- $\varepsilon$  turbulence model was used. The governing equations were solved using Fluent ANSYS 15.0 software, based on the finite volume method. The optimal disposition and dimension of the VG was determined through a parametric study. The results show that the vortex generators can effectively improve the aerodynamic performance of the NACA 4415 profile in the range of high attack angles. On the other hand, an optimal position and the optimal dimensions of the VG was obtained.

## 2. Mathematical modeling

In this study, the fluid was considered Newtonian and incompressible. The fluid flow was assumed three-dimensional, turbulent and stationary. The continuity and the momentum conservation equations are given by:

$$\frac{\partial U_i}{\partial X_i} = 0 \quad (1)$$

$$U_j \frac{\partial U_i}{\partial X_j} = -\frac{1}{\rho} \frac{\partial P}{\partial X_i} + \frac{1}{\rho} \frac{\partial}{\partial X_j} \left( \mu \frac{\partial U_i}{\partial X_j} - \overline{\rho U_i U_j} \right) \quad (2)$$

The Reynolds stress equation is given by:

$$-\overline{\rho U_i U_j} = \mu_t \left( \frac{\partial U_i}{\partial X_j} + \frac{\partial U_j}{\partial X_i} \right) - \frac{2}{3} \rho k \delta_{ij} \quad (3)$$

where  $\delta_{ij}$  is the Kronecker function

$\mu_t$  is the eddy viscosity which is given by:

$$\mu_t = \rho C_\mu \frac{k^2}{\varepsilon} \quad (4)$$

The Realizable k- $\varepsilon$  turbulence model was chosen. It is a mathematical approach similar to k- $\varepsilon$  standard model and is characterized by the following equations:

$$\frac{\partial}{\partial t} (\rho k) + \frac{\partial}{\partial X_j} (\rho k U_j) = \frac{\partial}{\partial X_j} \left[ \left( \mu + \frac{\mu_t}{\sigma_k} \right) \frac{\partial k}{\partial X_j} \right] + P_k + P_b - \rho \varepsilon - Y_M + S_k \quad (5)$$

$$\frac{\partial}{\partial t} (\rho \varepsilon) + \frac{\partial}{\partial X_j} (\rho \varepsilon U_j) = \frac{\partial}{\partial X_j} \left[ \left( \mu + \frac{\mu_t}{\sigma_\varepsilon} \right) \frac{\partial \varepsilon}{\partial X_j} \right] + \rho C_1 S_\varepsilon - \rho C_2 \frac{\varepsilon^2}{k + \sqrt{\nu \varepsilon}} + C_{1\varepsilon} \frac{\varepsilon}{k} C_{3\varepsilon} P_b + S_\varepsilon \quad (6)$$

The constant values are given by:

$$C_{1\varepsilon} = 1.44, C_2 = 1.9, \sigma_k = 1, \sigma_\varepsilon = 1.2$$

The Aerodynamic coefficients are:

The pressure coefficient

$$C_p = (P - P_0) / (\rho U_\infty^2 / 2) \quad (7)$$

The lift coefficient

$$C_L = F_y / (\rho S U_\infty^2 / 2) \quad (8)$$

The drag coefficient

$$C_D = F_x / (\rho S U_\infty^2 / 2) \quad (9)$$

The boundary conditions are:

At the inlet, the velocity is equal to 21m/s, corresponding to a 215000 Reynolds number.

At the outlet, the following parameters are imposed:

$$\frac{\partial U}{\partial y} = 0, \quad \frac{\partial P}{\partial y} = 0, \quad \frac{\partial T}{\partial y} = 0 \quad (10)$$

At the top and bottom of the domain symmetrical conditions are imposed.

### 3. Numerical resolution procedure

The governing equations were solved with Fluent ANSYS 15.0 software, based on the finite volume method. The SIMPLE algorithm was used for the resolution of the pressure-velocity coupling. The pressure-based solver, the standard pressure interpolation scheme and the implicit formulation method were chosen. For more accurate results, the second-order upwind scheme was adopted in the momentum equation discretization.

#### 3.1. Grid independence study

A grid independence study was conducted to select an optimum mesh number which guarantees that the solution is independent of the mesh resolution. The independence from the mesh size was evaluated through the lift and drag coefficients variations. For that purpose, two different grids (tetrahedral and quadratic grids) with different refinement were tested. The grids were generated by Gambit mesh generator software. The grid details are presented in Table 1.

Mesh type	Elements' numbers	Nodes' numbers
Tetrahedral 1	438493	82776
Tetrahedral 2	711851	127690
Tetrahedral 3	2482909	431264
Tetrahedral 4	6286679	1076933
Quadratic 1	2863978	3086286
Quadratic 2	529416	589350

**Table 1.** Mesh details

The lift and drag coefficients variations with the angle of attack obtained by simulation were compared to Fouatih et al. (2016) results. The comparisons are presented in Figures 1 and 2.

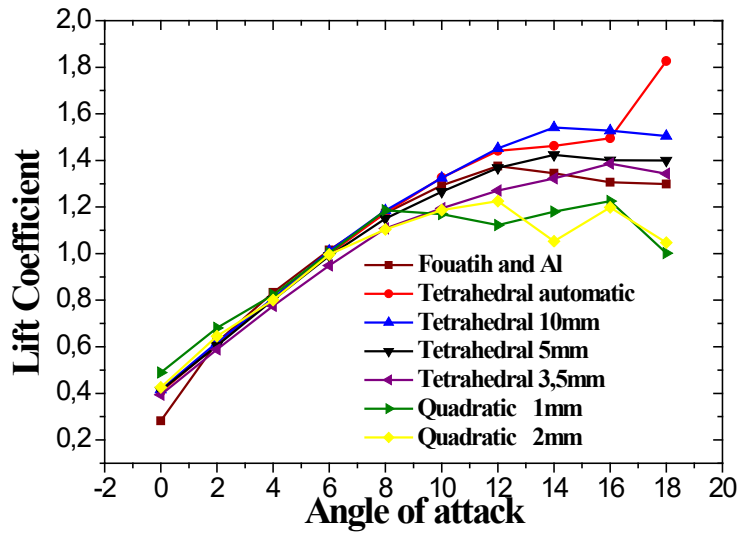


Fig. 1. Lift coefficient calculated numerically for different grids compared to Fouatih et al. (2016) results

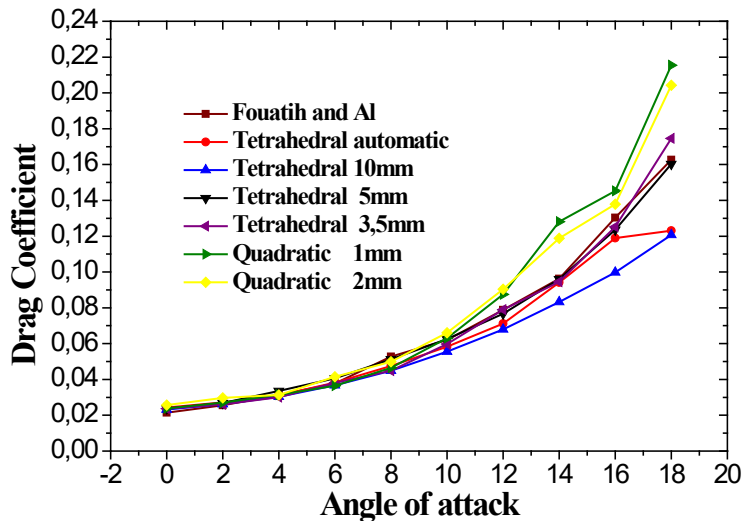
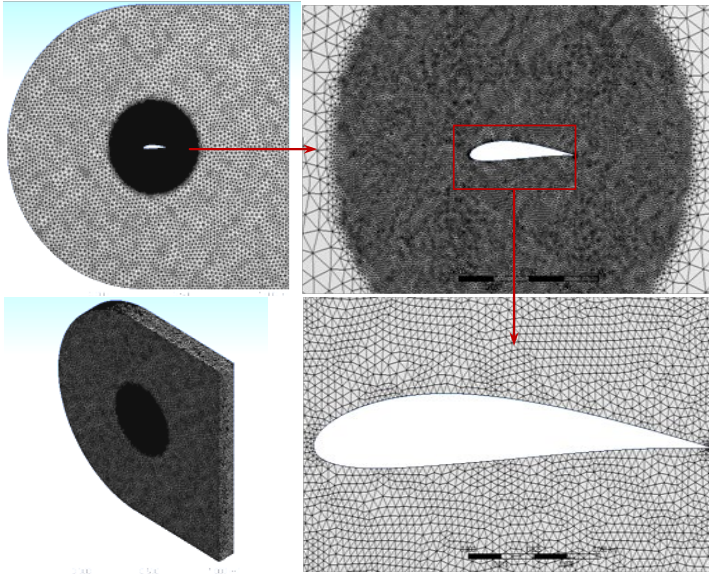


Fig. 2. Drag coefficient calculated numerically for different grids compared to Fouatih et al. (2016) results

We note a discrepancy between Fouatih et al. (2016) results and quadratic grid 1 and 2 for the attack angle  $\beta > 8^\circ$ , and tetrahedral grid 1 and 2, for the attack angle  $\beta > 14^\circ$ . There is a good agreement between Fouatih et al. (2016) results and tetrahedral grid 3 and 4. Finally, Tetrahedral 3 was adopted in the simulation because of its lowest number of elements and nodes, and hence the lowest computation time. The chosen mesh is shown in Figure 3.



**Fig. 3.** The used mesh

### 3.2. Validation of the numerical procedure

The lift and drag coefficients variations with the attack angle obtained in our numerical procedure was compared to these obtained by other authors. Zhen et al. (2011) obtained their results for a Reynolds number equal to 213000. Pope et al. (1966) results were obtained for a Reynolds number equal to 250000. The results of Fouatih et al. (2016) and Efstratios (1988) were obtained for a Reynolds number equal to 200000. The numerical results in our simulation were obtained for Reynolds number equal to 2150000. The lift and drag coefficients variations with the angle of attack are shown respectively in Figures 4 and 5. It is clear that a good agreement is reached between the numerical results and these in the literature.

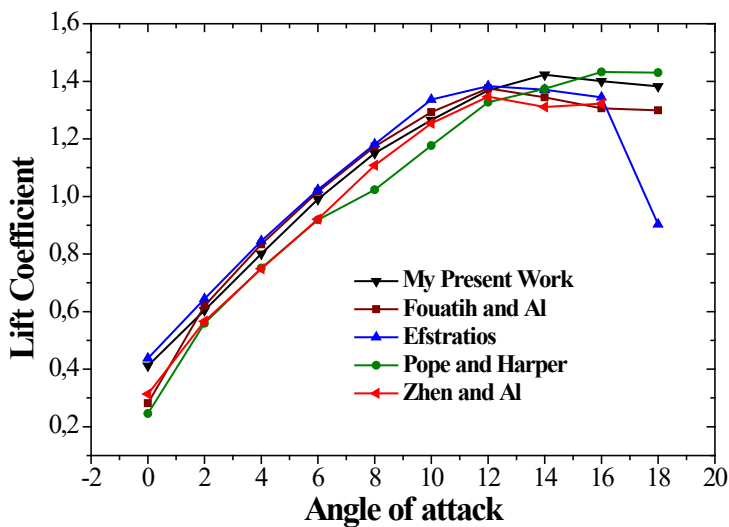


**Fig. 4.** Lift coefficient calculated numerically compared to these obtained by different authors

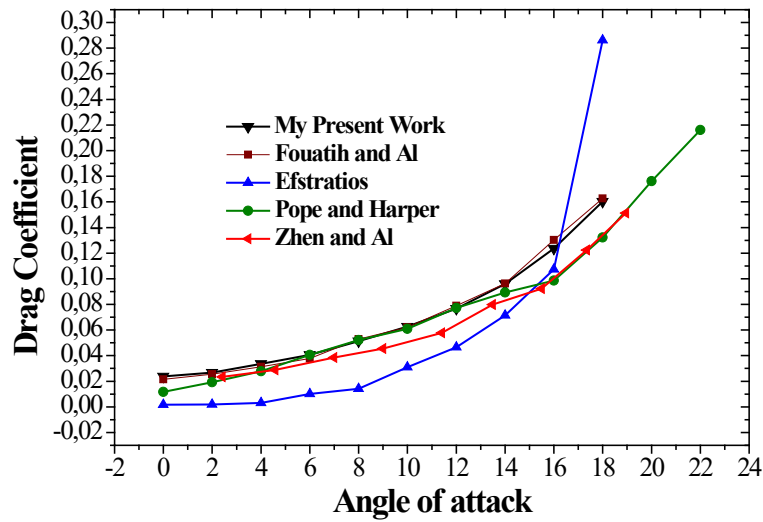


Fig. 5. Drag coefficient calculated numerically compared to these obtained by different authors

#### 4. Results and discussions

The aim of this study was the use Gothic-shaped vortex generators to improve the aerodynamic performances of the NACA 4415 profile. The vortex generators were used at the extrados of the profile as shown in Figure 6.

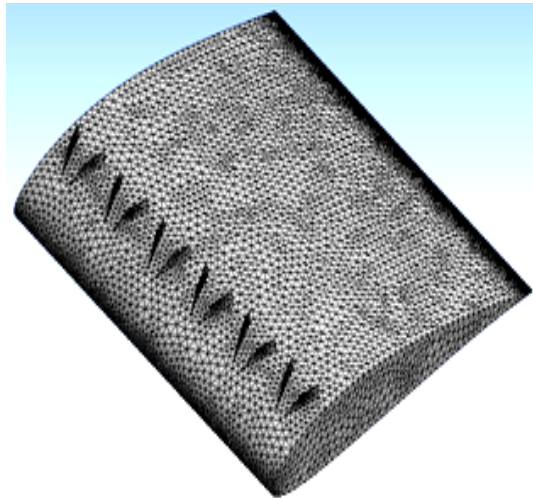
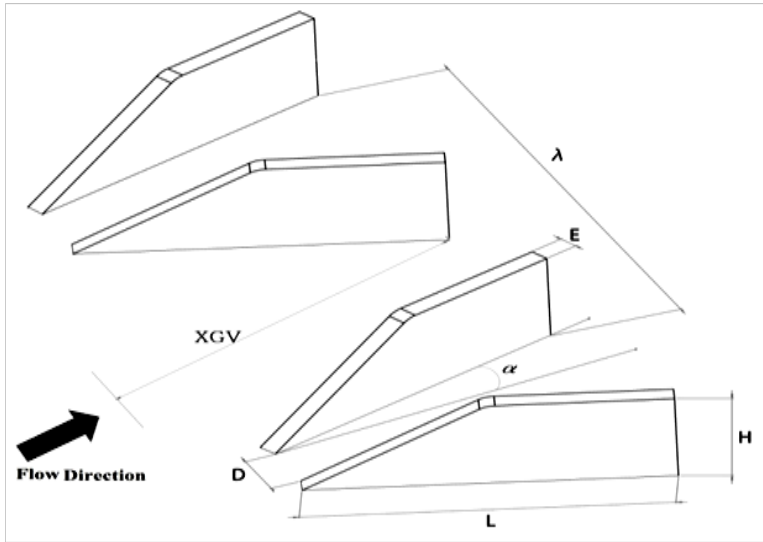


Fig. 6. Vortex generators position on the NACA 4415 profile

A parametric study was carried out based on different geometric parameter of the used vortex generators (Figure 7): thickness ( $E$ ), height ( $H$ ), length ( $L$ ), aspect ratio ( $r = H/L$ ), the wind incidence angle ( $\alpha$ ) and the vortex generators position relative to the chord ( $XVG$ ). This study was carried out with the NACA 4415 profile with a wingspan of 0.15 m and a chord of 0.15 m.



**Fig. 7.** Vortex generators geometric parameters

Geometric parameters		Dimensions			
Thickness	E (mm)	0.2	0.5	1	/
Height	H (mm)	3	5	7	
Length	L (mm)	10	15	20	
Aspect ratio	$r = H/L$	0.25	0.33	0.35	0.5
Incidence angle	$\alpha$ ( $^\circ$ )	15	19	20	21
Position	XVG (%)	20	30	40	/
Distance	$\lambda$ (mm)	25	25	25	25

**Table 2.** Vortex generators geometric dimensions

#### 4.1. Effect of the vortex generators

The effect of the vortex generators on the performances of the NACA 4415 profile is illustrated in Figures 8 and 9. The vortex generators have the following geometric dimensions:  $E = 0.2$  mm,  $r = 0.33$ ,  $\alpha = 20^\circ$  and  $XGV = 20\%$ . The results show an increase in the profile lift coefficient with VG beyond the attack angle  $10^\circ$  compared to the profile without VG. However, the drag coefficient is not significantly affected.

The Lift-to-Drag coefficient ratio ( $C_L/C_D$ ) illustrated in Figure 10 shows that the efficiency of the VG appears for high attack angles ( $10^\circ \leq \beta \leq 18^\circ$ ).

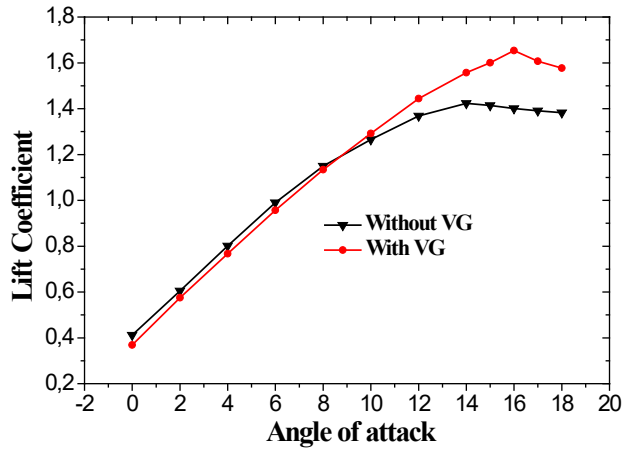


Fig. 8. Lift coefficient variations with and without vortex generators

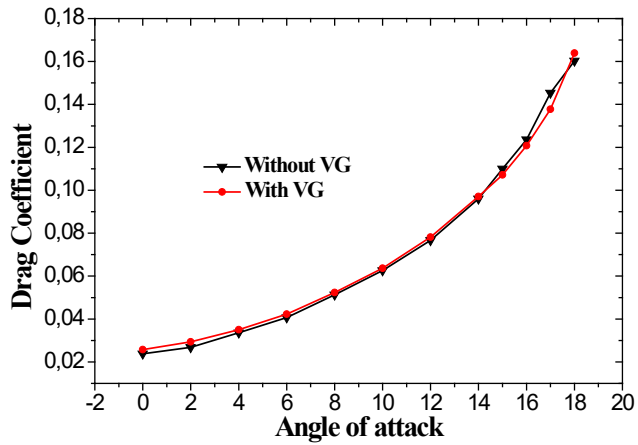


Fig. 9. Drag coefficient variations with and without vortex generators

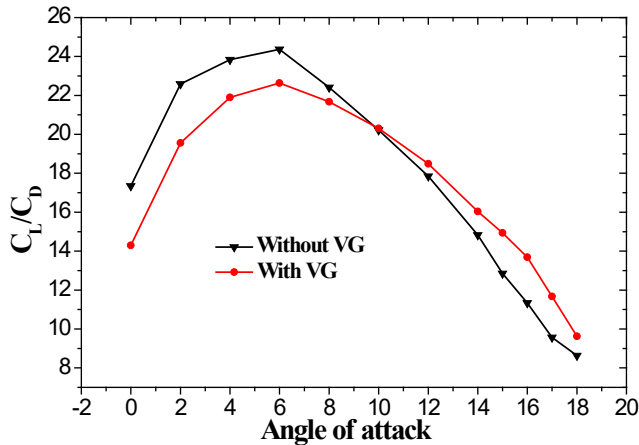


Fig. 10. Lift-to-Drag coefficient ratio with and without vortex generators

#### 4.2. Parametric study

For the parametric study, different geometric parameters were tested to determine the vortex generators disposition and dimensions which give optimal aerodynamic performances of the NACA 4415 profile. For this purpose, six parameters were tested (Table 2).

##### 4.2.1. Thickness effects

Figures 11 and 12 show the effect of the vortex generators thickness on the lift and drag coefficients respectively. The results were obtained for  $XVG = 20\%$ ,  $\alpha = 20^\circ$  and  $r = 0.33$ .

High values of the lift coefficient were obtained for the VG with a thickness of 0.2 mm for high attack angles ( $10^\circ \leq \beta \leq 18^\circ$ ). The drag coefficient corresponding to this thickness value ( $E = 0.2$  mm) remained lower than the other values ( $E = 0.5$  and 1 mm).

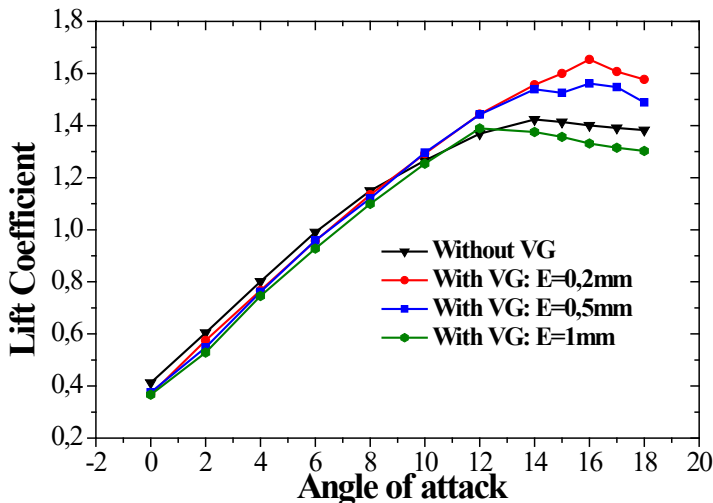


Fig. 11. Lift coefficient for different vortex generators thickness

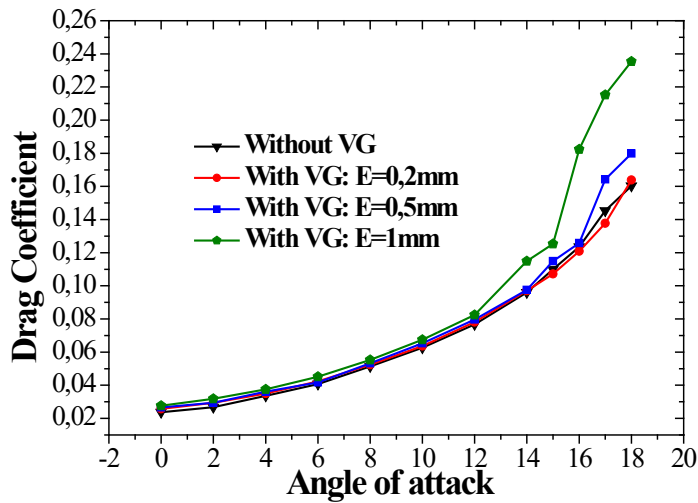


Fig. 12. Drag coefficient for different vortex generators thickness

The VG with 1 mm thickness are not suitable; they lead to a reduction in the aerodynamic performance of the profile for high attack angles ( $12^\circ \leq \beta \leq 18^\circ$ ) compared to the profile without VG. The Lift-to-Drag coefficient ratio (Figure 13) shows that the VG with a thickness of 0.2 mm optimal aerodynamic performances appear in the range of high attack angles ( $10^\circ \leq \beta \leq 18^\circ$ ) compared to other values. In the range of low attack angles ( $0^\circ \leq \beta \leq 10^\circ$ ) the optimal aerodynamic performances were obtained for the NACA 4415 profile without VG. The VG with 1 mm thickness leads to the degradation of the profile aerodynamic performances.

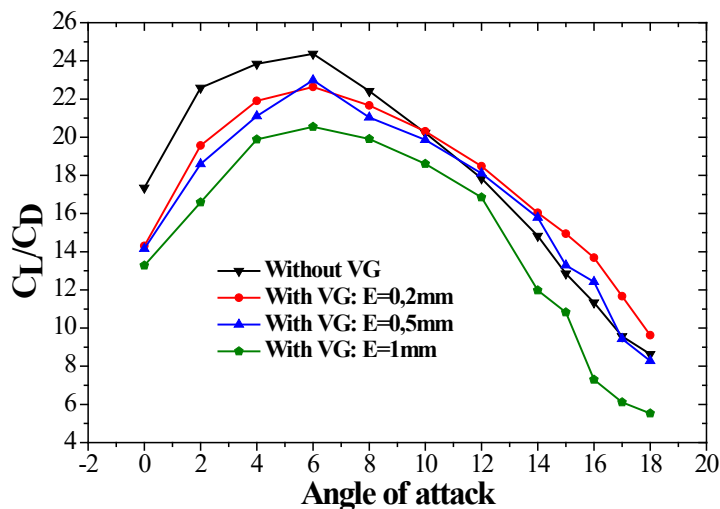


Fig. 13. Lift-to-Drag coefficient for different vortex generators thickness

#### 4.2.2. Height effects

The effect of the vortex generators height on the lift and drag coefficients are shown in Figures 14 and 15, respectively. The vortex generators length was taken equal to 15 mm. It is clear that

the best performances (high values of the lift coefficient and low ones of the drag coefficient) are obtained for the VG with 5 mm height for high attack angles ( $10^\circ \leq \beta \leq 18^\circ$ ).

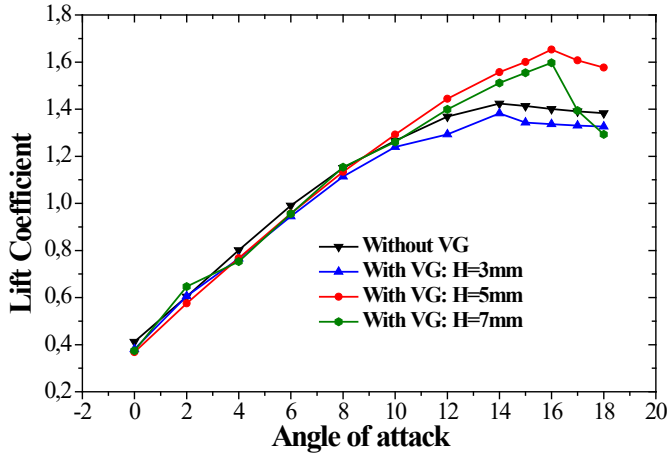


Fig. 14. Lift coefficient for different vortex generators heights

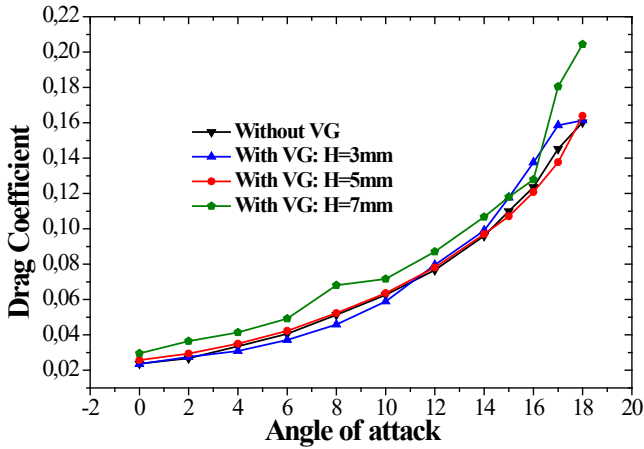


Fig. 15. Drag coefficient for different vortex generators heights

The Lift-to-Drag coefficient ratio (Figure 16) shows that the optimal aerodynamic performances of the profile are obtained with a VG heights equal to 5 mm for high attack angles ( $10^\circ < \beta \leq 18^\circ$ ). For low attack angles ( $3^\circ \leq \beta \leq 10^\circ$ ) the optimal aerodynamic performances are obtained for 3 mm VG heights. The NACA 4415 profile without VG is better for very small attack angles ( $0^\circ \leq \beta \leq 3^\circ$ ). VG with 7 mm thickness leads to the profile aerodynamic performances degradation.

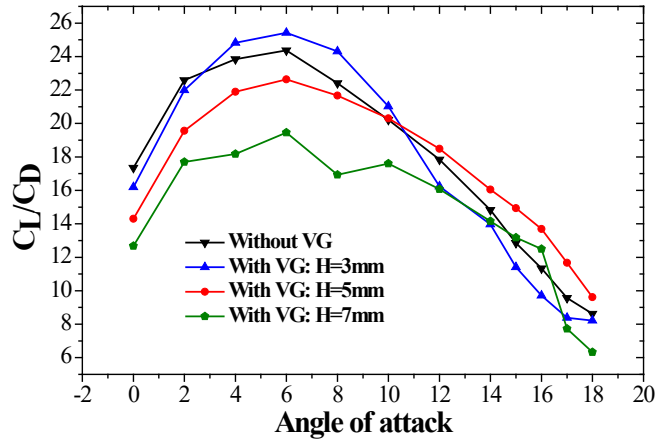


Fig. 16. Lift-to-Drag coefficient for different vortex generators heights.

#### 4.2.3. Length effects

Figures 17 and 18 illustrate the effect of the vortex generators length on the lift and drag coefficients respectively. We can see that, the optimal profile performances are obtained for a VG length equal to 15 mm for high attack angles ( $10^\circ < \beta \leq 18^\circ$ ). In figure 19, the Lift-to-Drag coefficient ratio variation shows that the optimal aerodynamic performances of the profile are obtained with a VG length equal to 15 mm for high attack angles ( $10^\circ < \beta \leq 18^\circ$ ). For low attack angles ( $0^\circ \leq \beta \leq 10^\circ$ ) the NACA 4415 profile without VG has better aerodynamic performances.

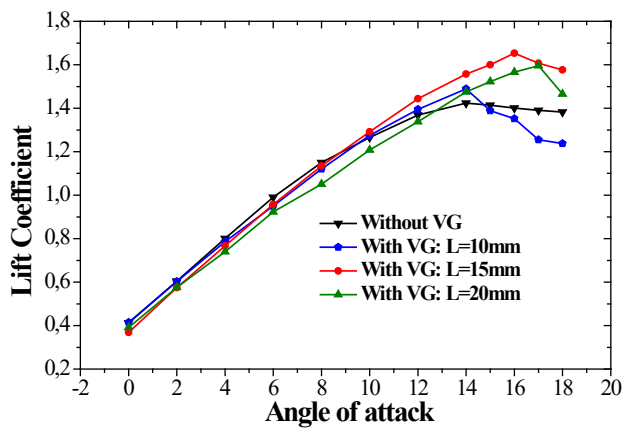


Fig. 17. Lift coefficient for different vortex generators lengths.

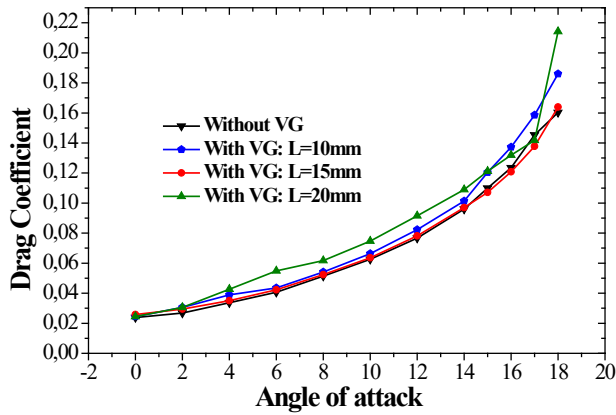


Fig. 18. Drag coefficient for different vortex generators lengths

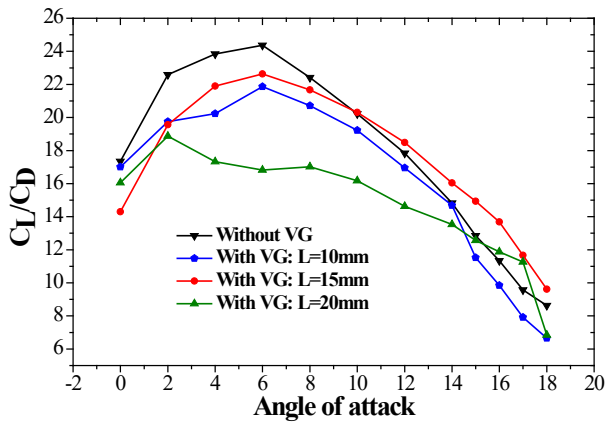


Fig. 19. Lift-to-Drag coefficient for different vortex generators lengths

#### 4.2.4. Incidence angle effects

The incidence angle effects on lift and drag coefficients are shown in Figures 20 and 21, respectively. We can notice that, for low attack angles ( $0^\circ \leq \beta \leq 10^\circ$ ) the angle of incidence has little effect on the profile aerodynamic performances. For high attack angles ( $10^\circ < \beta \leq 18^\circ$ ), the profile optimal performances are obtained for the incidence angle  $\alpha = 20^\circ$ .

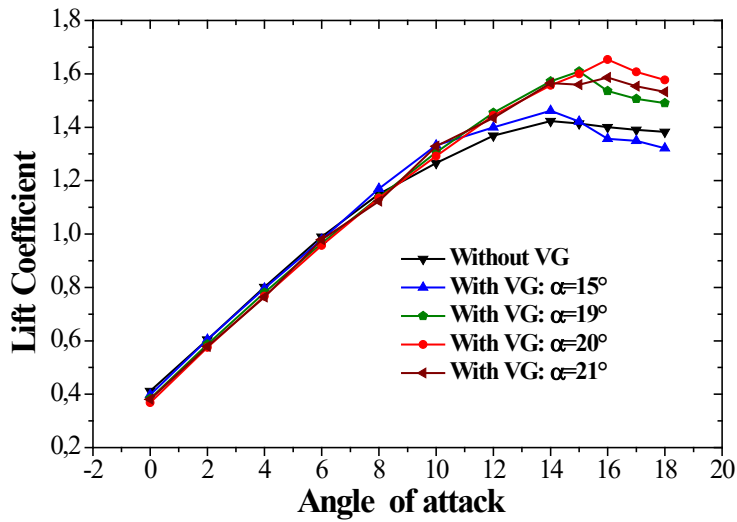


Fig. 20. Lift coefficient for different vortex generators incidence angles

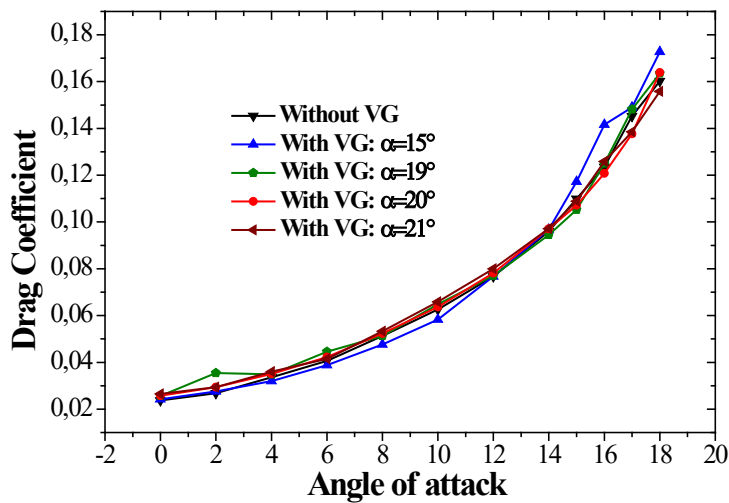


Fig. 21. Drag coefficient for different vortex generators incidence angles

Regarding the Lift-to-Drag coefficient ratio (Figure 22), we can notice that:

- In the range of very low attack angles ( $0^\circ \leq \beta \leq 3^\circ$ ) the NACA 4415 profile without VG has the best aerodynamic performances.
- For low attack angles ( $3^\circ \leq \beta \leq 12^\circ$ ), the incidence angle  $\alpha = 15^\circ$  has the best performances.
- For attack angles ( $12^\circ \leq \beta \leq 15^\circ$ ), the incidence angle  $\alpha = 19^\circ$  gives the best performances.
- For high attack angles ( $15^\circ < \beta \leq 18^\circ$ ), the incidence angle  $\alpha = 20^\circ$  gives the best performances.

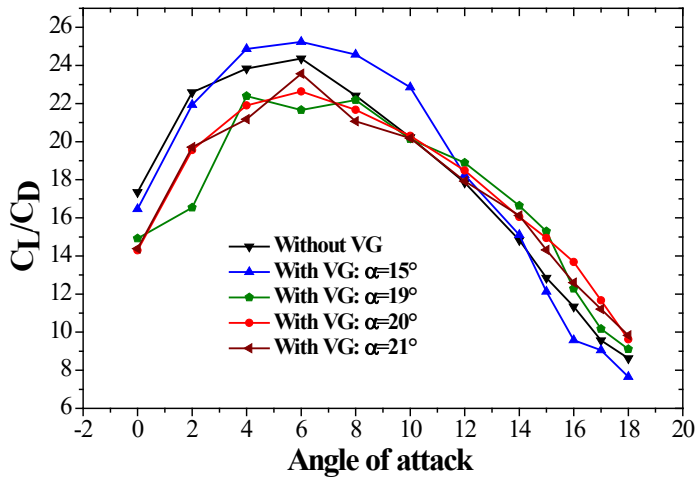


Fig. 22. Lift-to-Drag coefficient for different vortex generators incidence angles

#### 4.2.5 The XVG position effects

The effect of the position of the vortex generators relative to the chord (XVG) has been studied for a thickness  $E = 0.2$  mm, an incidence angle  $\alpha = 20^\circ$  and an aspect ratio  $r = 0.33$ . The results are shown in Figures 23 and 24 representing the lift and drag coefficients variation respectively. We can notice that, in the range of low angles of attack ( $0^\circ \leq \beta \leq 10^\circ$ ) the position XVG has a little effect on the profile aerodynamic performances. However, for of high attack angles ( $10^\circ < \beta \leq 18^\circ$ ) the XVG position has a significant effect. Regarding the Lift-to-Drag coefficient ratio (Figure 25), we can notice that:

- For low attack angles ( $0^\circ \leq \beta \leq 8^\circ$ ) the NACA 4415 profile without VG has the best aerodynamic performances.
- For attack angles ( $8^\circ \leq \beta \leq 12^\circ$ ), the position  $XGV = 40\%$  has the best performances.
- For attack angles ( $12^\circ < \beta \leq 14^\circ$ ), the position  $XGV = 30\%$  gives the best performances.
- For high attack angles ( $14^\circ < \beta \leq 18^\circ$ ), the position  $XGV = 20\%$  gives the best performances.

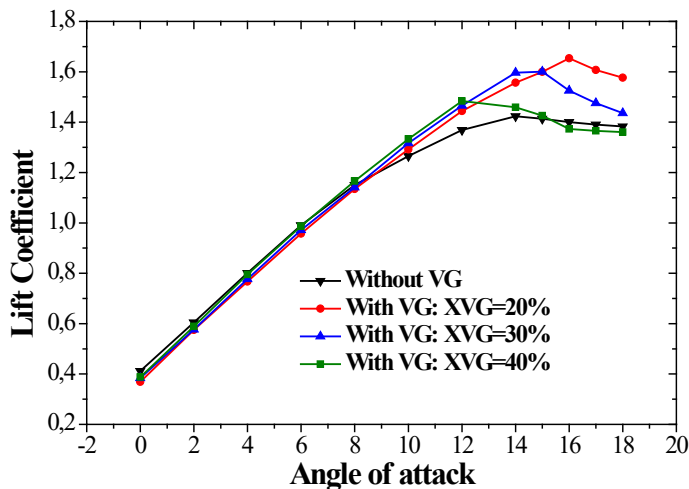


Fig. 23. Lift coefficient for different XVG positions of the vortex generators

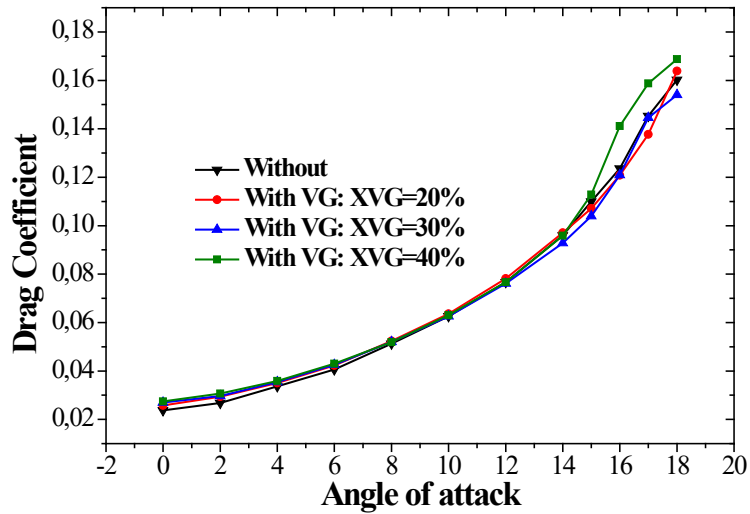


Fig. 24. Drag coefficient for different XVG positions of the vortex generators

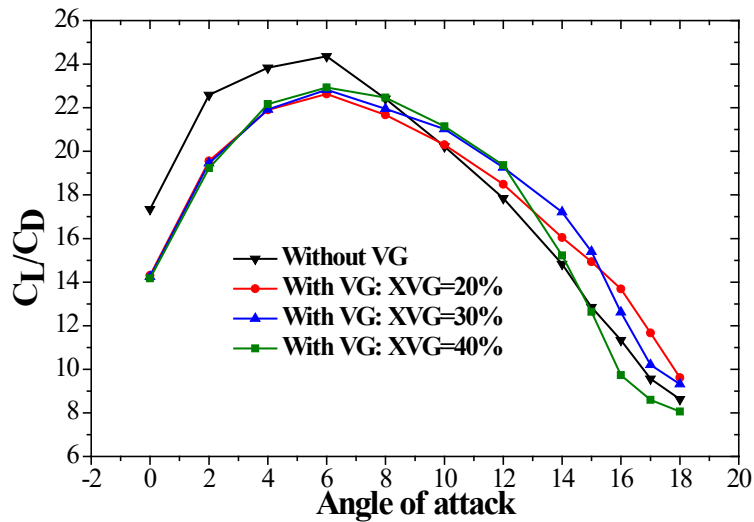


Fig. 25. Lift-to-Drag coefficient for different XVG positions of the vortex generators

#### 4.2.6. The aspect ratio effects

The effect of the vortex generators aspect ratio on the lift and drag coefficients are shown in Figures 26 and 27. The results show that, in the range of low attack angles ( $0^\circ \leq \beta \leq 10^\circ$ ), the NACA 4415 profile without VG has the best aerodynamic performances. However, in the range of high attack angles ( $10^\circ \leq \beta \leq 17^\circ$ ) the optimum aerodynamic performances have been obtained for the aspect ratio  $r = 0.33$ . This finding is confirmed by the lift-to-drag coefficient illustrated in Figure 28.

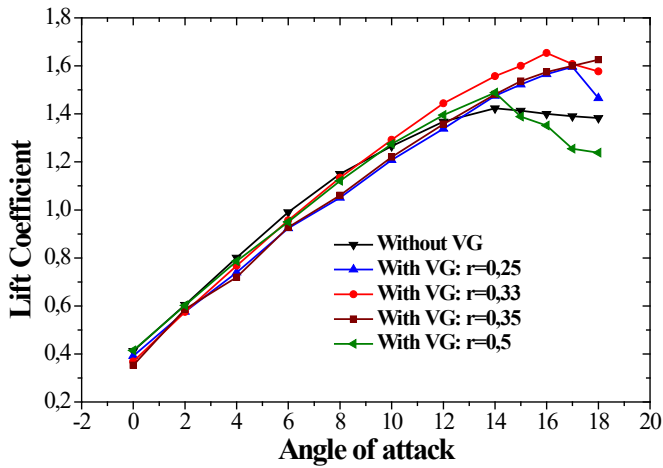


Fig. 26. Lift coefficient for different aspect ratio of the vortex generators

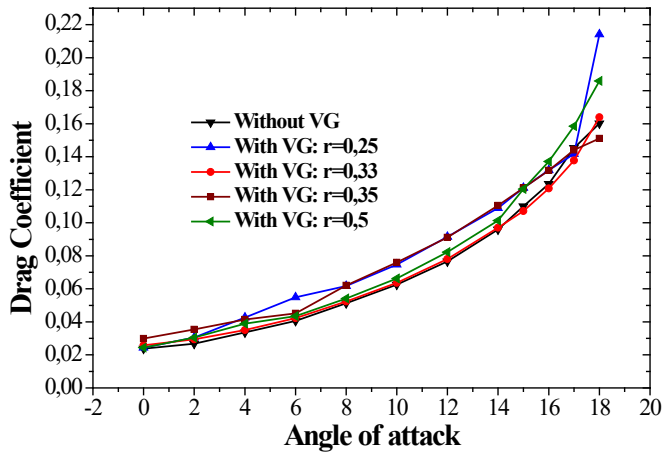


Fig. 27. Drag coefficient for different aspect ratio of the vortex generators

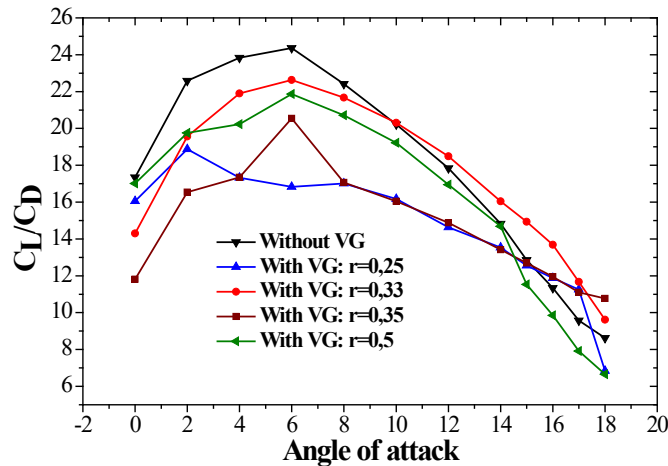


Fig. 28. Lift-to-Drag coefficient for different aspect ratio of the vortex generators

We can conclude from this parametric study that the position and the dimensions of the vortex generators affect the aerodynamic performances of NACA4415 profile. In the range of low attack angles ( $0^\circ < \beta \leq 10^\circ$ ), the NACA 4415 profile without VG has the best aerodynamic performances. In the range of high attack angles ( $10^\circ < \beta \leq 18^\circ$ ), the efficiency of the VG is preponderant. The optimal dimensions of the VG are:  $E = 0.2$  mm,  $H = 5$  mm,  $L = 15$  mm,  $r = 0.33$  and  $\alpha = 20^\circ$ .

Concerning the optimal XVG position, the best performances of the profile were obtained for the position  $XVG = 40\%$  in the range of attack angles ( $8^\circ \leq \beta \leq 12^\circ$ ). In the range of attack angles ( $12^\circ < \beta \leq 14^\circ$ ), the position  $XVG = 30\%$  gives the best performances and in the range of high attack angles ( $14^\circ < \beta \leq 18^\circ$ ), the position  $XVG = 20\%$  gives the best performances.

The velocity and pressure contours with and without vortex generators are shown in Figures 29 and 30, respectively. The results are presented for an attack angle equal to  $14^\circ$  and for VG optimal dimensions ( $E = 0.2$  mm,  $H = 5$  mm,  $L = 15$  mm,  $XVG = 20\%$  and  $r = 0.33$ ). The attached VG can significantly affect the pressure distribution at the profile intrados and extrados. This improves the aerodynamic performance of the profile. On the other hand, the presence of the VG can avoid flow separation at the trailing edge and prevents pressure losses in the trailing edge reducing the drag force.

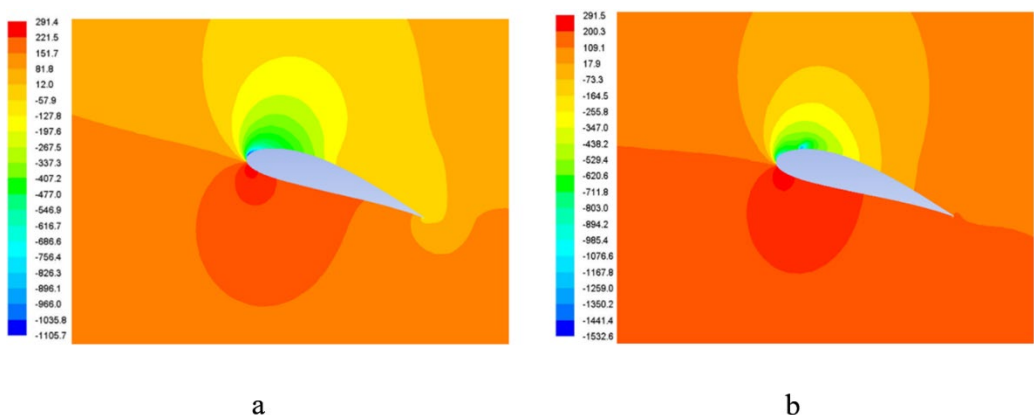
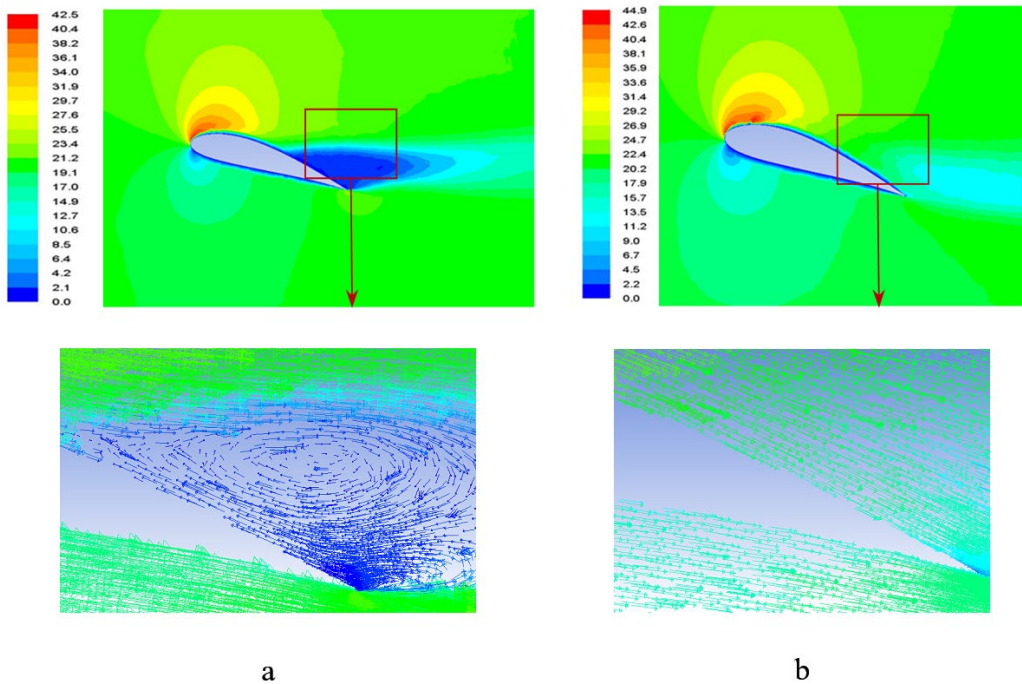


Fig. 29. Pressure contours around the NACA4415 profile: (a) without VG, (b) with VG.



**Fig. 30.** Velocity contours around the NACA4415 profile: (a) without VG (b) with VG.

## 5. Conclusions

In this paper, the improvement of aerodynamic performances of the airfoil NACA 4415 by passive flow control using vortex generators was investigated numerically. The numerical simulation procedure was validated by comparing the results with other authors' results. The results show that the vortex generators improve effectively the lift coefficient of the profile for high attack angles. For low attack angles, the best aerodynamic performances were obtained for the airfoil without vortex generators. The parametric study for different geometric parameters led to optimal dimensions of the vortex generators. An optimal position relative to the chord of the profile ( $XVG$ ) was found:

For attack angles ( $8^\circ \leq \beta \leq 12^\circ$ ), the profile best performances were obtained for the position  $XGV = 40\%$ .

For attack angles ( $12^\circ < \beta \leq 14^\circ$ ), the position  $XGV = 30\%$  gave the best performances and for high attack angles ( $14^\circ < \beta \leq 18^\circ$ ), the position  $XGV = 20\%$  led to the best performances of the airfoil.

## References

Agarwal S, Kumar P (2016). Numerical Investigation of Flow Field and Effect of Varying Vortex Generator Location on Wing Performance. *American Journal of Fluid Dynamics*. 6(1): 11-19.

- Belamadi R, Djemili A, Ilinca A, Mdouki R (2016). Aerodynamic performance analysis of slotted airfoils for application to wind turbine blades. *Journal of Wind Engineering and Industrial Aerodynamics*. 151: 79-99.
- Benazieb B, Nemouchi Z (2015). Simulation d'un écoulement d'air projeté sur un profil de pale d'éolienne avec générateurs de vortex. *Revue des Energies Renouvelables*. 18(1): 127-141.
- Cai C, Zuo Z, Liu S, Maeda T (2017). Effect of a single leading-edge protuberance on NACA 634-021 airfoil performance. *Journal of Fluids Engineering*. 140(2): 021108- 021115.
- Efstratiou S (1988). The aerodynamic performance of the NACA-4415 aerofoil section at low Reynolds numbers. *M. Sc. Thesis. Department of Aerospace Engineering, University of Glasgow, Scotland*.
- Forster K, White T (2014). Numerical Investigation into Vortex Generators on Heavily Cambered Wings. *AIAA Journal*. 52(5): 1059-1071.
- Fouatih O, Medale M, Imine O, Imine B (2016). Design optimization of the aerodynamic passive flow control on NACA 4415 airfoil using vortex generators. *European Journal of Mechanics-B/Fluids*. 56: 82-96.
- Fouatih O (2016). Interaction entre un tourbillon et une couche limite : Application au générateur de tourbillon sur une aile. *PHD Thesis, University of Science and Technology, Oran, Alegria*.
- Godard G, Stanislas M (2006). Control of a decelerating boundary layer. Part 1: Optimization of passive vortex generators. *Aerospace Science and Technology*. 10(3): 181-191.
- Gopinathan V T, Ganesh M (2015). Passive Flow Control over NACA0012 Aerofoil using Vortex Generators. *International Journal of Engineering Research & Technology*. 4(9): 674-678.
- Huang J B (2010). Study of control effects of vortex generators on a supercritical wing. *Science China Technological Sciences*. 53: 2038-2048.
- Kumar G, Narayanan K, Aravindhkumar S, KishoreKumar S (2016). Comparative Analysis of Various Vortex Generators for a NACA 0012 Aerofoil. *International Journal of Innovative Studies in Sciences and Engineering Technology*. 2(5): 3-6.
- Kumar V, Bogadi S (2011). Effect of micro-vortex generator in hypersonic inlet. *International Journal of Appl. Res. Mech. Eng*. 1: 10-13.
- Lu F K, Li Q, Shih Y, Pierce A, Liu C (2011). Review of micro vortex generators in high-speed flow. in: *49th AIAA Aerospace Sciences Meeting Including the New Horizons Forum and Aerospace Exposition. Orlando, Florida, USA*.
- Mdouki R (2017). Passive Control of Laminar Bubble Separation for S809 Wind Turbine Airfoil via Slot. *Proc. 23rd French Congress of Mechanics, Lille, France*.
- Menghu H, Jun L, Zhongguo N, Hua L, Guangyin Z, Weizhuo H (2015). Aerodynamic performance enhancement of a flying wing using nanosecond pulsed DBD plasma actuator. *Chinese Journal of Aeronautics*. 28(1): 377-384.
- Moshfeghi M, Shams S, Hur N (2017). Aerodynamic performance enhancement analysis of horizontal axis wind turbines using a passive flow control method via split blade. *Journal of Wind Engineering and Industrial Aerodynamics*. 167: 148-159.
- Mustak R, Khan M, Molla M (2017). Design and construction of NACA-4415 airfoil with various shaped surface modifications. *Asia Pacific Journal of Engineering Science and Technology*. 3(1): 28-38.
- Pope A, Harper J (1966). Low Speed Wind Tunnel Testing. *John Wiley and Sons, New York, USA*.
- Sartor F, Losfeld G, Leclaire B, Bur R (2013). Characterization by PIV of the effect of vortex generators in a transonic separated flow. *Proc. 10th International Symposium on Particle Image Velocimetry PIV13, Delft, Netherlands*.
- Shehataa A, Xiao Q, Saqr K, Naguib A, Alexander D (2017). Passive flow control for aerodynamic performance enhancement of airfoil with its application in Wells turbine-Under oscillating flow condition. *Ocean Engineering*, 136: 31-53.

- Skarolek V, Karabelas S (2016). Energy efficient active control of the flow past an aircraft wing: RANS and LES evaluation. *Applied Mathematical Modelling*. 40(2): 700-725
- Součkov N, Simurda D, Popelka L (2009). Control of boundary layer separation on flapped airfoil with low-profile vortex generator. *Proc. Colloquium Fluid Dynamics, Institute of Thermomechanics AS CR, Prague, Czech Republic*.
- Tebbiche H, Boutoudj M (2014). Aerodynamic drag reduction by turbulent flow control with vortex generators. *Proc. 5th International Symposium on Aircraft Materials, Marrakech, Morocco*.
- Tebbiche H, Boutoudj M S (2014). Optimized vortex generators in the flow separation control around a NACA 0015 profile. *Proc. 9th International Conference on Structural Dynamics, Porto, Portugal*.
- Tebbiche H and Boutoudj M (2015). Passive Control on the NACA 4412 Airfoil and Effects on the Lift. *Springer, International Publishing, Switzerland*.
- Tebbiche H (2016). Evolution et contrôle de la couche limite dans le cas de profil NACA, PHD thesis. *Mouloud Mammeri University of Tizi Ouzou, Alegria*.
- Veldhuis L, Jansen D, Haddar J, Correale G (2012). Novel Passive and Active Flow Control for High Lift. *Proc. 28th International Congress of the Aeronautical Sciences, Brisbane, Australia*.
- Vidhyasri E, Narentharan T E, Naveenkumar M, Murali M. (2017). Design and Analysis of Vortex Generator to Reduce Drag Force in Sedan Vehicle. *International Journal of Advanced Science and Engineering Research*. 2: 287-301.
- Wu J M, Tao W Q (2012). Effect of longitudinal vortex generator on heat transfer in rectangular channels. *Applied Thermal Engineering*. 37: 67-72.
- Zhen T K, Zubair M, Ahmad K A (2011). Experimental and numerical investigation of the effects of passive vortex generators on aludra UAV performance. *Chinese Journal of Aeronautics*. 24(5): 577-583.